remote sensing

MDPI

Article

Optimal Configuration of Array Elements for Hybrid Distributed PA-MIMO Radar System Based on Target Detection

Cheng Qi, Junwei Xie, Haowei Zhang *, Zihang Ding and Xiao Yang

Air and Missile Defense College, Air Force Engineering University, Xi'an 710051, China
* Correspondence: zhw_xhzf@163.com

Abstract: This paper establishes a hybrid distributed phased array multiple-input multiple-output (PA-MIMO) radar system model to improve the target detection performance by combining coherent processing gain and spatial diversity gain. First, the radar system signal model and array space configuration model for the PA-MIMO radar are established. Then, a novel likelihood ratio test (LRT) detector is derived based on the Neyman–Pearson (NP) criterion in a fixed noise background. It can jointly optimize the coherent processing gain and spatial diversity gain of the system by implementing subarray level and array element level optimal configuration at both receiver and transmitter ends in a uniform blocking manner. On this basis, three typical optimization problems are discussed from three aspects, i.e., the detection probability, the effective radar range, and the radar system equipment volume. The approximate closed-form solutions of them are constructed and solved by the proposed quantum particle swarm optimization-based stochastic rounding (SR-QPSO) algorithm. Through the simulations, it is verified that the proposed optimal configuration of the hybrid distributed PA-MIMO radar system offers substantial improvements compared to the other typical radar systems, detection probability of 0.98, and an effective range of 1166.3 km, which significantly improves the detection performance.

Keywords: radar resource optimization; target detection; array element configuration; PA-MIMO radar

Citation: Qi, C.; Xie, J.; Zhang, H.; Ding, Z.; Yang, X. Optimal Configuration of Array Elements for Hybrid Distributed PA-MIMO Radar System Based on Target Detection. *Remote Sens.* **2022**, *14*, 4129. https://doi.org/10.3390/rs14174129

Academic Editors: Jingwei Xu, Keqing Duan, Weijian Liu and Xiongpeng He

Received: 21 July 2022
Accepted: 17 August 2022
Published: 23 August 2022

1. Introduction

Challenges, such as the diversity of modern radar targets and the complexity of the battlefield environment, have exposed the inadequacy of existing radar regimes and detection technologies [1–3]. To cope with complex targets and environments [4] and seek breakthroughs in target detection theory and technology [5], regime modification and resource management for radar are being continuously and intensively carried out [6–8]. Maximizing the cognitive operation capability [9,10], optimizing the utilization of available resources [11,12], and improving the target detection capability of radar systems are fundamental topics and practical and urgent tasks faced in the field of radar information processing and optimal resource management [13,14].

The multiple-input multiple-output (MIMO) radar system has received extensive attention as a novel radar system recently for its potential to significantly improve radar detection performance in a number of important application areas, including autonomous driving and imaging systems [1,15]. Generally, the MIMO radar has two kinds of configurations, a collocated MIMO system and distributed MIMO system [16]. The collocated MIMO system mainly uses modulated detection signals to achieve superior waveform diversity, and its transmit apertures are all collocated on a single tower or platform, whereas the transmit apertures of the distributed MIMO system are located on widely separated platforms. Thus, it can obtain the diversity gain of echo signals brought by angular extension and effectively overcome target scintillation to improve detection performance [17].

However, the MIMO radar transmits orthogonal waveforms, which leads to it losing the coherent array-processing-gain advantage enjoyed by conventional phased-array radar

systems [18]. In principle, both coherent processing gain and spatial diversity gain can improve radar detection performance [19]. However, reference [20–22] shows that both distributed MIMO radars with diversity gain and phased array radars with coherent processing gain are non-optimal. Therefore, it is far from sufficient to simply increase the total resources of the radar system without considering the cooperation between individual array elements. How to harmoniously utilize the spatial diversity gain and phase coherence gain and optimize the ratio of the two gains to maximize the overall performance of the system is an urgent and complex issue to be solved.

The trade-off between coherent integration via DBF and incoherent integration via spatial diversity becomes a new direction in radar design. Furthermore, the proposal of a phased-array multiple-input multiple-output (PA-MIMO) radar has created a new avenue for the development of the MIMO radar [23,24]. The hybrid distributed PA-MIMO radar is a combination of traditional phased array radar and MIMO radar technology. It utilizes the coherent processing gain and spatial diversity gain, which are obtained simultaneously from the coherence of array elements signal within the subarray and the orthogonality of the inter-subarray signal, respectively. Therefore, the hybrid distributed PA-MIMO radar system can maintain the advantages of distributed MIMO radar while having the benefits of coherent processing of phased-array radar, and it is a compromise and effective implementation scheme [25,26]. Therefore, array element configuration optimization is a critical issue for radar resource management, and its research is of high relevance.

Numerous scholars have conducted in-depth studies on the array elements configuration of radar systems. The division of the transmitting array into multiple overlapped subarrays in [27] improved the angular resolution and target detection capacity, and [28] studied the optimal sparse array optimization configuration problem in the presence of multiple sources of interest (SOI). In [29], the authors proposed an algorithm for the joint arrangement of transmitter and receiver in the distributed MIMO radar to improve the localization accuracy. There is also a solid research foundation for improving system detection performance through array element configuration optimization. In [30], the target detection capability is optimized by deploying the array elements in space through an exhaustive method and completing the power allocation through a waterfilling-type algorithm. In [25], the transmit arrays are divided into many uniformly overlapping subarrays to obtain coherent processing gain and waveform diversity gain simultaneously, and the theoretical derivation and simulation experiments demonstrate the superiority of PA-MIMO radar. However, there is a lack of systematic research on the problem of element configuration optimization. The simple division schemes are not satisfactory in many performance indicators. Therefore, from the perspective of radar equipment development, there is an urgent need for research on optimal element configuration and processing [31].

Aiming at solving the issues above, the optimal allocation of two gains in a MIMO multisite radar system (MSRS) is proposed in [20] from the receiver side through the configuration of the spatial location of the array elements. In [32,33], the optimal configuration of digital array radar is investigated to study the effect of array space configuration optimization on radar system performance improvement from the receiver side. However, few references simultaneously consider the allocation and optimization of coherent processing gain and spatial diversity gain in a PA-MIMO radar system from both the transmitter and receiver sides.

In this paper, we establish the radar system signal model and array space configuration model for a hybrid distributed PA-MIMO radar. Then, the likelihood ratio test (LRT) detector in Neyman–Pearson (NP) criterion with respect to the array space configuration is derived. On this basis, three typical optimization problems are discussed, i.e., maximizing the detection probability, maximizing the effective radar range, and minimizing the radar system equipment volume for a given detection requirement. In this regard, the approximate closed-form solutions are constructed and solved by the proposed quantum particle swarm optimization-based stochastic rounding (SR-QPSO) algorithm to obtain the optimal strategy for the array element configuration. Finally, the solution realizes the optimal

cooperation among the array elements to improve the radar detection performance based on the total amount of existing radar resources.

The main contributions and results of this paper are summarized as follows.

(1) We formulated the closed form element configuration problem as an optimization model for the hybrid distributed PA-MIMO radar based on NP criterion. In this study, the spatial configuration of the array elements is implemented through uniform division of the target scattering matrix, and the likelihood ratio test detector is derived from this for target detection of the hybrid distributed PA-MIMO radar.
(2) We proposed an efficient quantum particle swarm optimization-based stochastic rounding (SR-QPSO) algorithm to cope with the integer programming closed-form approximation optimization problem. The formulated configuration scheme is a two integer-variable optimization problem, which contains a transmitting end blocking variable and a receiving end blocking variable. To obtain the optimal solution, we extended the basic QPSO algorithm to a stochastic rounding method combined with the cyclic minimization algorithm (CMA).
(3) We presented three numerical simulation results to demonstrate the theoretical findings and validate the effectiveness of the proposed optimization scheme. Moreover, the three simulations also illustrate the elements configuration optimization achieves a better detection performance improvement for the hybrid distributed PA-MIMO radar in three totally different aspects: Detection Probability, Effective Radar Range and System Equipment Volume.

The rest of the paper is organized as follows. The hybrid distributed PA-MIMO system model, along with the system configuration based on the diversity conditions, are demonstrated in Section 2. Section 3 derives the LRT detector from the NP criterion based on the signal processing flow of the hybrid distributed PA-MIMO radar. In Section 4, three optimization scenarios are considered and propose a solution algorithm based on integer programming. Section 5 presents numerical results and analysis. Section 6 discusses the simulation result and presents some further qualitative analysis. Finally, Section 7 concludes the paper.

2. System Model

2.1. Proposed Hybrid Distributed PA-MIMO Radar System Signal Model

A hybrid distributed PA-MIMO radar observation model is shown in Figure 1, which uses M transmitting array elements and N receiving array elements in a two-dimensional plane x-o-y to simultaneously transmit orthogonal waveform signals and receive the target echo signal. Under this approach, each sub-array of the radar system is a phased array radar, and the MIMO mode is conducted between different sub-arrays. In addition, the transient transmitted power of each element is P_t, the transmitting antenna gain is G_t, the receiving antenna gain is G_r, and the transmitting signal wavelength is λ. Then, according to the primary radar equation and the MIMO radar signal model [19], the signal scattered by the target located at (x_0, y_0) and received by the n-th receiving element can be expressed as:

$$r_n(t) = \sum_{m=1}^{M} \sqrt{\frac{P_t G_{mt} G_{nr} \lambda^2}{(4\pi)^3 R_m^2 R_n^2 L} \sigma_{nm}} e^{j\varphi_{nm}} s_m(t - \tau_{mn}) + n_n(t) \quad (1)$$

where $s_m(t)$ presents the narrowband signal transmitted by the m-th transmitting array element, which satisfies the MIMO radar orthogonal signal condition $\int s_k(t) s_l^*(t) dt = \delta_{kl}$, where δ_{kl} is the Kronecker Delta function, $(\cdot)^*$ represents conjugate transpose operation, and $\|s_m(t)\|^2 = 1$. The term L is the system loss, P_t is the constant pulse transmitting power of radar, φ_{nm} is the phase difference caused by the spatial configuration of radar elements in multi-channel sampling, and $\tau_{mn} = (R_m + R_n)/c$ represents the time delay caused by the sum of the distance R_m from the m-th transmitting array element to the target centroid and the distance R_n from the target to the n-th receiving array element in the n-mth

channel, wherein the constant value c is the speed of light. Additionally, $n_n(t)$ represents the receiver thermal noise in the n-th receiving element. The fluctuating value σ_{nm} is the radar cross-section (RCS) observed by the m-nth channel, which obeys a complex Gaussian distribution that $\sigma_{nm} \sim N(0, \sigma^2)$. In addition, the distance between the target and each element of the radar system satisfies the far-field condition, while the maximum distance between the elements is much smaller, that is $R_m = R_n = R$.

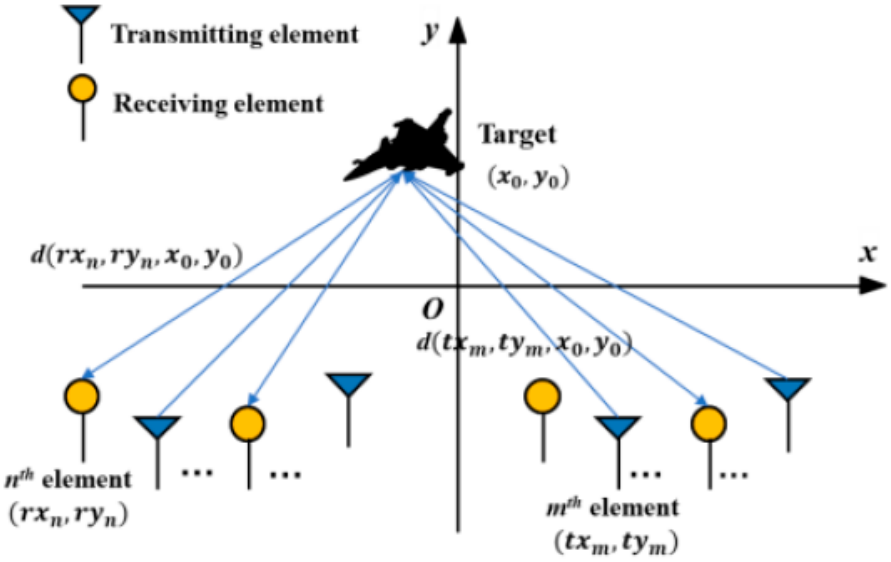

Figure 1. Hybrid distributed PA-MIMO radar configuration.

Furthermore, the signal transmitted by M transmitting array elements and scattered by the target, and ultimately received by N receiving array elements can be expressed as:

$$\begin{cases} \mathbf{r}(t) = \sqrt{P_t} diag(\mathbf{a}) \mathbf{H} diag(\mathbf{b}) \mathbf{s}(t - \tau_{mn}) + \mathbf{n}(t) \\ [\mathbf{H}]_{mn} = \alpha_{nm} = \sqrt{\frac{G_{mt} G_{nr} \lambda^2 \sigma_{nm}}{(4\pi)^3 R^4 L}} \end{cases} \tag{2}$$

where $\mathbf{H}$ represents the $N \times M$ dimensional coefficient matrix of the target scattering coefficient corresponding to the independent channel of the radar system. Additionally, α_{mn} can be regarded as a complex zero-mean Gaussian-distributed variable with a variance σ_T^2. $\mathbf{a} = \left[1, e^{-j\phi_2}, \cdots, e^{-j\phi_N}\right]^T$ denotes the receiving steering vector of the radar system, $\mathbf{b} = \left[1, e^{-j\psi_2}, \cdots, e^{-j\psi_M}\right]^T$ is the transmitting steering vector and satisfies $\varphi_{nm} = \psi_m + \phi_N$. And the vector $\mathbf{s}(t) = [s_1(t), s_2(t), \cdots, s_M(t)]^T$ is the transmitted signal. $\mathbf{n}(t) = [n_1(t), \cdots, n_N(t)]^T \sim N(0, \sigma_n^2 \mathbf{I}_N)$ represents an additive white Gaussian noise vector, where $\mathbf{I_N}$ is a $N \times N$ dimensional matrix.

2.2. Hybrid Distributed PA-MIMO Radar System Configuration

The target motion model is described by the constant acceleration (CA) model:

The correlation between the elements of the target scattering coefficient matrix can be adjusted by changing the distance between each subarray of the radar system [17], thus changing the processing mode of the echo signal in the radar system. Without loss of generality, the correlation of the spatial signal is defined by the array element spacing d as [34]:

$$d \geq \lambda R / D \tag{3}$$

where D is the tangential length of the target.

The spatial configuration of the hybrid distributed PA-MIMO radar, and the allocation of the proportions of the two gains in the radar system essentially change the correlation of elements in the target scattering coefficient matrix $\mathbf{H}$. If the array elements' spacing does

not satisfy the space diversity condition in (3), the sub-arrays are combined into a phased array radar; on the contrary, the sub-arrays follow the MIMO radar signal processing mechanism. Therefore, changing the distance between the radar elements ensures that the corresponding target scattering coefficients are perfectly correlated or uncorrelated.

Once the target scattering coefficients α_{lk} and α_{nm} are completely uncorrelated, the radar system possesses an angular broadening of the space target, resulting in a spatial diversity gain. Accordingly, when α_{lk} and α_{nm} are entirely correlated, the radar system performs coherent processing on r_{lk} and r_{nm} to improve the signal-to-noise ratio (SNR) of the target echo signals. Herein, the target scattering coefficient matrix is reorganized and divided according to the correlation of each channel, and the target scattering coefficient matrix $\hat{\mathbf{H}}$ will be reconstructed as (4) after the configuration.

$$\hat{\mathbf{H}} = \begin{bmatrix} \mathbf{H}_{11} & \cdots & \mathbf{H}_{1\hat{M}} \\ \vdots & \ddots & \vdots \\ \mathbf{H}_{\hat{N}1} & \vdots & \mathbf{H}_{\hat{N}\hat{M}} \end{bmatrix}_{\hat{N}\times\hat{M}} \tag{4}$$

where target scattering coefficient matrix sub-block $\mathbf{H}_{\hat{n}\hat{m}}$ contains $a_{\hat{m}} \times b_{\hat{n}}$ coherent processing channel. Figure 2 intuitively illustrates the array element configuration of the hybrid distributed PA-MIMO radar. M transmitting array elements and N receiving array elements are reorganized and divided into $\hat{N}$ and $\hat{M}$ subarrays, respectively. The $\hat{N}$ transmitter subarrays and the $\hat{M}$ receiver subarrays perform coherent processing as a phased array radar. Simultaneously, each subarray also transmits and receives independent orthogonal signals as a MIMO radar for diversity processing so that the radar system has coherent processing gain and space diversity gain at the same time.

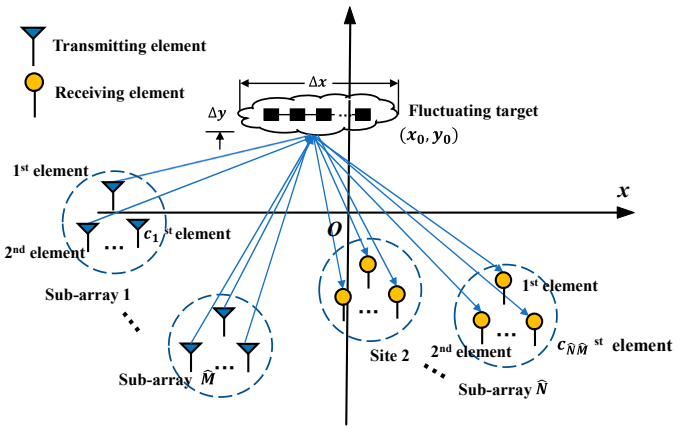

Figure 2. Optimal array elements configuration of hybrid distributed PA-MIMO radar.

Spatial diversity processing can improve the detection performance by increasing the number of independent channels, and coherent processing improves the detection performance by increasing the detection SNR of each channel. By dividing the target scattering coefficient matrix into blocks, the proportion of space diversity gain and coherent processing gain in the radar system is coordinated and allocated to optimize the target detection performance of the radar system.

3. Hybrid Distributed PA-MIMO Radar System with Optimal Configuration

3.1. Signal Processing Flow of Hybrid Distributed Phased Array MIMO Radar

For the proposed hybrid distributed PA-MIMO radar system, Figure 3 shows the signal processing schematic. $\hat{M}$ orthogonal transmit signals are scattered by the target to $\hat{N}$ receiver subarrays. Subsequently, matched filter banks are used to generate $\hat{N} \times \hat{M}$ independent channel outputs. Then, coherent accumulation and space-time compensation are

performed within the subarray, and finally, signal sampling and likelihood ratio detection are performed [35].

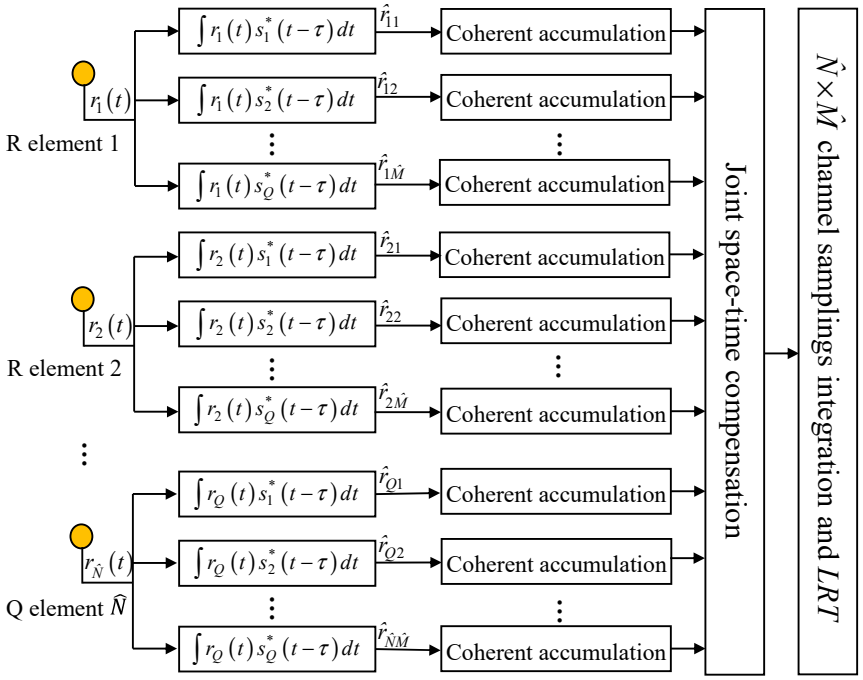

Figure 3. Signal processing flowchart of hybrid distributed PA-MIMO radar. Where * denotes convolution operation.

Then, for the detection unit containing a target, the $\hat{N} \times \hat{M}$ channel samplings may be approximated as:

$$\hat{r}_{\hat{n}\hat{m}}(t) = a_{\hat{m}} b_{\hat{n}} \sqrt{P_t} \hat{\alpha}_{\hat{n}\hat{m}} + n_{\hat{n}\hat{m}} \tag{5}$$

where $a_{\hat{m}}$ represents the number of transmitter array elements contained in the reorganized subarray and $b_{\hat{n}}$ represents the number of transmitter array elements. $n_{\hat{n}\hat{m}}$ is the white Gaussian-distributed noise samplings of the n-mth channel with auto-correlation $b_{\hat{n}}\sigma_n^2$. Since the subarray configuration follows the non-overlapping principle, it satisfies:

$$\begin{cases} M = \sum\limits_{\hat{m}=1}^{\hat{M}} a_{\hat{m}} \\ N = \sum\limits_{\hat{n}=1}^{\hat{N}} b_{\hat{n}} \end{cases} \tag{6}$$

Therefore, the SNR corresponding to the sampling value of each subarray can be approximated as:

$$\rho_{\hat{n}\hat{m}} = \frac{(a_{\hat{m}} b_{\hat{n}})^2 T_s \sigma_T^2}{b_{\hat{n}} \sigma_n^2} = a_{\hat{m}}^2 b_{\hat{n}} \rho_0 \tag{7}$$

where T_s is the duration of transmitting pulse. For simplicity, we define $\rho_0 = \sigma_T^2 T_s / \sigma_n^2$ as the reference channel SNR, which indicates the SNR provided by a single independent channel on the target at a distance R_0.

3.2. LRT Detector of the Hybrid Distributed PA-MIMO Radar System

The spatial configuration makes the outputs of each subarray independent and orthogonal to each other. Assuming that the received noise level is known, each echo signal $\hat{\mathbf{r}} = \left[\hat{r}_{11}, \hat{r}_{12}, \cdots, \hat{r}_{\hat{N}\hat{M}}\right]_{1\times\hat{N}\hat{M}}$ is an independent identically distributed (IID) complex Gaus-

sian random vector. And the square-law detection outputs of different stations of the radar system are given by:

$$\mathbf{X} = \left[X_{11}, X_{12}, \cdots, X_{\hat{N}\hat{M}}\right]_{1\times\hat{N}\hat{M}} \tag{8}$$

where $X_{\hat{n}\hat{m}} = \|\hat{r}_{\hat{n}\hat{m}}\|^2$

So, the target detection problem can be expressed as:

$$\begin{cases} \mathcal{H}_0 : \hat{\mathbf{r}}(t) = \mathbf{n}(t) & \text{, Target does not exist at delay} \tau. \\ \mathcal{H}_1 : \hat{\mathbf{r}}(t) = \hat{\mathbf{H}}\mathbf{s}(t) + \mathbf{n}(t) & \text{, Target exists at delay} \tau. \end{cases} \tag{9}$$

and the probability density function can be expressed as:

$$\begin{cases} f(\mathbf{X}|\mathcal{H}_0) = \prod\limits_{\hat{n}=1}^{\hat{N}} \prod\limits_{\hat{m}=1}^{\hat{M}} \left[\frac{1}{b_{\hat{n}}\sigma_n^2} \exp\left(-\frac{X_{\hat{n}\hat{m}}}{b_{\hat{n}}\sigma_n^2}\right)\right] \\ f(\mathbf{X}|\mathcal{H}_1) = \prod\limits_{\hat{n}=1}^{\hat{N}} \prod\limits_{\hat{m}=1}^{\hat{M}} \left[\frac{1}{b_{\hat{n}}\sigma_n^2(1+\rho_{\hat{n}\hat{m}})} \exp\left(-\frac{X_{\hat{n}\hat{m}}}{b_{\hat{n}}\sigma_n^2(1+\rho_{\hat{n}\hat{m}})}\right)\right] \end{cases} \tag{10}$$

The hybrid distributed PA-MIMO radar LRT detector is represented as:

$$\mathbb{T}_{\text{HDPM}} = \frac{f(\mathbf{X}|\mathcal{H}_1)}{f(\mathbf{X}|\mathcal{H}_0)} \underset{\mathcal{H}_0}{\overset{\mathcal{H}_1}{\gtrless}} \eta_0 \tag{11}$$

and

$$\mathbb{T}_{\text{HDPM}} = \frac{f(\mathbf{X}|\mathcal{H}_1)}{f(\mathbf{X}|\mathcal{H}_0)} = \prod_{\hat{n}=1}^{\hat{N}} \prod_{\hat{m}=1}^{\hat{M}} \left[\frac{1}{1+\rho_{\hat{n}\hat{m}}} exp\left(\frac{\rho_{\hat{n}\hat{m}} X_{\hat{n}\hat{m}}}{b_{\hat{n}}\sigma_n^2(1+\rho_{\hat{n}\hat{m}})}\right)\right] \tag{12}$$

where $f(\cdot|\mathcal{H}_1)$ and $f(\cdot|\mathcal{H}_0)$, respectively, represent the conditional distribution density function under the two assumptions, $\mathbb{T}_{HPM}$ is the test statistic constructed from $X_{\hat{n}\hat{m}}$.

Further taking logarithms on both sides of (12), we have:

$$\ln(\mathbb{T}_{\text{HDPM}}) = \sum_{\hat{n}=1}^{\hat{N}} \sum_{\hat{m}=1}^{\hat{M}} \left[\ln\left(\frac{1}{1+\rho_{\hat{n}\hat{m}}}\right) + \frac{\rho_{\hat{n}\hat{m}}}{(1+\rho_{\hat{n}\hat{m}})} R_{\hat{n}\hat{m}}\right] \tag{13}$$

where

$$R_{\hat{n}\hat{m}} = \frac{X_{\hat{n}\hat{m}}}{b_{\hat{n}}\sigma_n^2} \sim \chi^2_{(2)} \quad \hat{m} = 1, 2, \ldots, \hat{M}; \hat{n} = 1, 2, \ldots, \hat{N} \tag{14}$$

$$\omega_{\hat{n}\hat{m}} = \frac{\rho_{\hat{n}\hat{m}}}{1+\rho_{\hat{n}\hat{m}}} \tag{15}$$

where $\chi^2_{(2)}$ represents a chi-square distribution with 2 degrees of freedom (DOF).

Herein, the LRT detector of the hybrid distributed PA-MIMO radar system can be expressed as:

$$\mathbb{T}_{\text{HDPM}} = \sum_{\hat{n}=1}^{\hat{N}} \sum_{\hat{m}=1}^{\hat{M}} [\omega_{\hat{n}\hat{m}} R_{\hat{n}\hat{m}}] \underset{\mathcal{H}_0}{\overset{\mathcal{H}_1}{\gtrless}} \eta_0 \tag{16}$$

where η_0 is a threshold according to the preset constant P_{F}.

(1) LRT Statistical Analysis under $\mathcal{H}_0$ Hypothesis

Under the hypothesis of $\mathcal{H}_0$, let $R'_{\hat{n}\hat{m}} = R_{\hat{n}\hat{m}}$ and $\omega'_{\hat{n}\hat{m}} = \rho_{\hat{n}\hat{m}}/(1+\rho_{\hat{n}\hat{m}})$, the LRT detector under the $\mathcal{H}_0$ hypothesis can be reformulated as:

$$\mathbb{T}_{\text{HDPM}|\mathcal{H}0} = \sum_{\hat{n}=1}^{\hat{N}} \sum_{\hat{m}=1}^{\hat{M}} \omega'_{\hat{n}\hat{m}} R'_{\hat{n}\hat{m}} \underset{\mathcal{H}_0}{\overset{\mathcal{H}_1}{\gtrless}} \eta_0 \tag{17}$$

where

$$R'_{\hat{n}\hat{m}} \sim \chi^2_{(2)} \tag{18}$$

where $R'_{\hat{n}\hat{m}}$ is a 2 DOF cardinality distribution variable, i.e., a standard exponential distribution variable [36]. For the test statistic $\mathbb{T}_{HPM|\mathcal{H}0}$, the weighted sum of the IID exponential distribution approximates the Gamma distribution with exponential scale parameters [37].

We have:

$$\mathbb{T}_{\mathrm{HDPM}|\mathcal{H}0} = \sum_{\hat{n}=1}^{\hat{N}} \sum_{\hat{m}=1}^{\hat{M}} \omega'_{\hat{n}\hat{m}} R'_{\hat{n}\hat{m}} \sim \Gamma\left(\frac{v_0}{2}, 2g_0\right) \tag{19}$$

where $\Gamma(\theta, \xi)$ is the gamma function, parameters θ and ξ represent the scale parameter and shape parameter of the gamma distribution, respectively, and v_0, g_0 are:

$$v_0 = \frac{2\left(\sum\limits_{\hat{n}=1}^{\hat{N}} \sum\limits_{\hat{m}=1}^{\hat{M}} \omega'_{\hat{n}\hat{m}}\right)^2}{\sum\limits_{\hat{n}=1}^{\hat{N}} \sum\limits_{\hat{m}=1}^{\hat{M}} \left(\omega'_{\hat{n}\hat{m}}\right)^2} = \frac{2\left(\sum\limits_{\hat{n}=1}^{\hat{N}} \sum\limits_{\hat{m}=1}^{\hat{M}} \frac{a^2_{\hat{m}} b_{\hat{n}t} \rho_0}{1+a^2_{\hat{m}} b_{\hat{n}t} \rho_0}\right)^2}{\sum\limits_{\hat{n}=1}^{\hat{N}} \sum\limits_{\hat{m}=1}^{\hat{M}} \left(\frac{a^2_{\hat{m}} b_{\hat{n}t} \rho_0}{1+a^2_{\hat{m}} b_{\hat{n}} \rho_0}\right)^2} \tag{20}$$

$$g_0 = \frac{\sum\limits_{\hat{n}=1}^{\hat{N}} \sum\limits_{\hat{m}=1}^{\hat{M}} \left(\omega'_{\hat{n}\hat{m}}\right)^2}{\sum\limits_{\hat{n}=1}^{\hat{N}} \sum\limits_{\hat{m}=1}^{\hat{M}} \omega'_{\hat{n}\hat{m}}} = \frac{\sum\limits_{\hat{n}=1}^{\hat{N}} \sum\limits_{\hat{m}=1}^{\hat{M}} \left(\frac{a^2_{\hat{m}} b_{\hat{n}t} \rho_0}{1+a^2_{\hat{m}} b_{\hat{n}} \rho_0}\right)^2}{\sum\limits_{\hat{n}=1}^{\hat{N}} \sum\limits_{\hat{m}=1}^{\hat{M}} \frac{a^2_{\hat{m}} b_{\hat{n}t} \rho_0}{1+a^2_{\hat{m}} b_{\hat{n}} \rho_0}} \tag{21}$$

(2) LRT Statistical Analysis under $\mathcal{H}_1$ Hypothesis

Under the hypothesis $\mathcal{H}_1$, with $R'_{\hat{n}\hat{m}} = R_{\hat{n}\hat{m}}/(1+\rho_{\hat{n}\hat{m}})$ and $\omega'_{\hat{n}\hat{m}} = (1+\rho_{\hat{n}\hat{m}})\omega_{\hat{n}\hat{m}} = \rho_{\hat{n}\hat{m}}$, the LRT detector of the system in hypothesis $\mathcal{H}_1$ can be re-expressed as:

$$\mathbb{T}_{\mathrm{HDPM}|\mathcal{H}1} = \sum_{\hat{n}=1}^{\hat{N}} \sum_{\hat{m}=1}^{\hat{M}} \omega'_{\hat{n}\hat{m}} R'_{\hat{n}\hat{m}} \underset{\mathcal{H}_0}{\overset{\mathcal{H}_1}{\gtrless}} \eta_0 \tag{22}$$

where

$$R'_{\hat{n}\hat{m}} \sim \chi^2_{(2)} \tag{23}$$

hen, we have:

$$\mathbb{T}_{\mathrm{HDPM}|\mathcal{H}1} = \sum_{\hat{n}=1}^{\hat{N}} \sum_{\hat{m}=1}^{\hat{M}} \omega'_{\hat{n}\hat{m}} R'_{\hat{n}\hat{m}} \sim \Gamma\left(\frac{v_1}{2}, 2g_1\right) \tag{24}$$

where

$$v_1 = \frac{2\left(\sum\limits_{\hat{n}=1}^{\hat{N}} \sum\limits_{\hat{m}=1}^{\hat{M}} \omega'_{\hat{n}\hat{m}}\right)^2}{\sum\limits_{\hat{n}=1}^{\hat{N}} \sum\limits_{\hat{m}=1}^{\hat{M}} \left(\omega'_{\hat{n}\hat{m}}\right)^2} = \frac{2\left(\sum\limits_{\hat{n}=1}^{\hat{N}} \sum\limits_{\hat{m}=1}^{\hat{M}} a^2_{\hat{m}} b_{\hat{n}} \rho_0\right)^2}{\sum\limits_{\hat{n}=1}^{\hat{N}} \sum\limits_{\hat{m}=1}^{\hat{M}} \left(a^2_{\hat{m}} b_{\hat{n}} \rho_0\right)^2} \tag{25}$$

$$g_1 = \frac{\sum\limits_{\hat{n}=1}^{\hat{N}} \sum\limits_{\hat{m}=1}^{\hat{M}} \left(\omega'_{\hat{n}\hat{m}}\right)^2}{\sum\limits_{\hat{n}=1}^{\hat{N}} \sum\limits_{\hat{m}=1}^{\hat{M}} \omega'_{\hat{n}\hat{m}}} = \frac{\sum\limits_{\hat{n}=1}^{\hat{N}} \sum\limits_{\hat{m}=1}^{\hat{M}} \left(a^2_{\hat{m}} b_{\hat{n}} \rho_0\right)^2}{\sum\limits_{\hat{n}=1}^{\hat{N}} \sum\limits_{\hat{m}=1}^{\hat{M}} a^2_{\hat{m}} b_{\hat{n}} \rho_0} \tag{26}$$

Therefore, considering Equations (16), (19) and (24) together, the LRT detector of the hybrid distributed PA-MIMO radar system is obtained as follows:

$$\mathbb{T}_{\mathrm{HDPM}} = \begin{cases} \Gamma\left(\frac{v_0}{2}, 2g_0\right), \mathcal{H}_0 \\ \Gamma\left(\frac{v_1}{2}, 2g_1\right), \mathcal{H}_1 \end{cases} \tag{27}$$

4. Optimization Model Establishment and Solution

4.1. Overview of the Optimization Problem for Hybrid Distributed PA-MIMO Radar Systems

Optimizing the array element configuration of the hybrid distributed PA-MIMO radar system aims to improve detection performance. Generally speaking, the evaluation criteria for target detection performance are as follows: detection probability P_{D} [38], detection range $R_{E\max}$ [20], resolution and SNR [39], etc. However, different optimal configuration strategies may be used for different optimization purposes. P_{D} is usually the most intuitive performance index used to describe the detection capability of the radar system. In addition, for a certain detection probability P_{D} and false alarm probability P_{FA}, the maximum operating distance $R_{E\max}$ of the radar system is pursued. Thirdly, it is also of great practical significance to reduce the amount of equipment of the radar system with the given false alarm probability P_{FA} and detection probability P_{D}. Therefore, according to system design purposes, the optimal configuration of the hybrid distributed PA-MIMO radar can be divided into the following three optimization problems.

Optimization problem 1: With a given $M \times N$ hybrid distributed PA-MIMO radar system, constant P_F and ρ_0, obtain the maximum target detection probability value, i.e., P_{D}, by optimizing the diversity vector $\boldsymbol{\beta} = \left(\hat{M}, a_1, \cdots, a_{\hat{M}}\right)$ and $\boldsymbol{\gamma} = \left(\hat{N}, b_1, \cdots, b_{\hat{N}}\right)$ based on the LRT detector of the radar system.

Optimization problem 2: With a given $M \times N$ hybrid distributed PA-MIMO radar system, constant P_F, P_D and ρ_0, obtain the maximum operating distance $R_{\max}$ by optimizing the diversity vector $\boldsymbol{\beta} = \left(\hat{M}, a_1, \cdots, a_{\hat{M}}\right)$ and $\boldsymbol{\gamma} = \left(\hat{N}, b_1, \cdots, b_{\hat{N}}\right)$ based on the LRT detector of the radar system.

Optimization problem 3: With a given constant P_F, P_D and ρ_0, minimize the equipment quantity of a hybrid distributed PA-MIMO radar by optimizing the diversity vector $\boldsymbol{\beta} = \left(\hat{M}, a_1, \cdots, a_{\hat{M}}\right)$ and $\boldsymbol{\gamma} = \left(\hat{N}, b_1, \cdots, b_{\hat{N}}\right)$ based on the LRT detector of the radar system.

4.2. Detection Performance Analysis of Typical Hybrid Distributed PA-MIMO Radar System

The above three optimization problems consider improving the target detection capability from different perspectives, but the core problem is to optimize the vector $\boldsymbol{\beta}$ and $\boldsymbol{\gamma}$. However, there is also a parameter coupling problem in the process of optimizing high-dimensional integer programming problems, which makes the analytical solution complex and impossible. To reduce the search time and solution complexity, array elements are divided into a certain number of non-overlapping subarrays, shown in (28).

$$\begin{cases} \hat{a}_m = \frac{M}{\hat{M}} \\ \hat{b}_n = \frac{N}{\hat{N}} \end{cases} \tag{28}$$

According to the array element configuration scheme, the hybrid distributed PA-MIMO radar system can be decomposed into four typical structures. These structures and their distribution of test statistics are shown below.

(1) **Distributed MIMO radar** with full diversity processing:

$$\mathbb{T}_{\mathrm{MIMO}} = \begin{cases} \Gamma\left(MN, \frac{2\rho_0}{1+\rho_0}\right) & , \mathcal{H}_0 \\ \Gamma(MN, 2\rho_0) & , \mathcal{H}_1 \end{cases} \tag{29}$$

(2) **Phased array radar** with full coherent processing:

$$\mathbb{T}_{\mathrm{PHASE}} = \begin{cases} \Gamma\left(1, \frac{2M^2N\rho_0}{1+M^2N\rho_0}\right) & , \mathcal{H}_0 \\ \Gamma\left(1, 2M^2N\rho_0\right) & , \mathcal{H}_1 \end{cases} \tag{30}$$

(3) **Multiple-input single-output (MISO) radar** with full diversity processing at the transmitter side and full coherent processing on the receiver side:

$$\mathbb{T}_{\text{SIMO}} = \begin{cases} \Gamma\left(M, \frac{2N\rho_0}{1+N\rho_0}\right) & , \mathcal{H}_0 \\ \Gamma(M, 2N\rho_0) & , \mathcal{H}_1 \end{cases} \tag{31}$$

(4) **Single-input multiple-output (SIMO) radar** with full diversity processing at the receiver side and coherent processing on the transmitter side. Similarly, the distribution of test statistics of these typical radars is obtained as:

$$\mathbb{T}_{\text{SIMO}} = \begin{cases} \Gamma\left(N, \frac{2M^2\rho_0}{1+M^2\rho_0}\right) & , \mathcal{H}_0 \\ \Gamma\left(N, 2M^2\rho_0\right) & , \mathcal{H}_1 \end{cases} \tag{32}$$

Thus, the P_D corresponding to each typical radar system with a certain P_{FA} can be given by:

$$P_{\text{D}-\text{MIMO}}(P_{\text{FA}}) = 1 - Q_{\chi^2_{(2MN)}}\left(\frac{Q^{-1}_{\chi^2_{(2MN)}}(1-P_{\text{FA}})}{1+\rho_0}\right) \tag{33}$$

$$P_{\text{D}-\text{PHASE}}(P_{\text{FA}}) = 1 - Q_{\chi^2_{(2)}}\left(\frac{Q^{-1}_{\chi^2_{(2)}}(1-P_{\text{FA}})}{1+M^2N\rho_0}\right) \tag{34}$$

$$P_{\text{D}-\text{MISO}}(P_{\text{FA}}) = 1 - Q_{\chi^2_{(2M)}}\left(\frac{Q^{-1}_{\chi^2_{(2M)}}(1-P_{\text{FA}})}{1+N\rho_0}\right) \tag{35}$$

$$P_{\text{D}-\text{SIMO}}(P_{\text{FA}}) = 1 - Q_{\chi^2_{(2N)}}\left(\frac{Q^{-1}_{\chi^2_{(2N)}}(1-P_{\text{FA}})}{1+M^2\rho_0}\right) \tag{36}$$

where $Q_{\chi^2_{(2MN)}}$ and $Q^{-1}_{\chi^2_{(2MN)}}$ represent the complementary cumulative distribution functions of chi-square with a $2MN-$DOF and its inverse function, respectively.

Clearly, array configuration can significantly affect the detection performance of the system. In addition, when M = N, the MISO radar, and SIMO radar test statistics have the same DOF, i.e., the same number of independent channels. However, the SIMO radar is M times the SNR of the MISO radar. Further analysis shows the optimal configuration of the system is $\hat{M} \times \hat{N}$ independent channels. So, the SNR gain can be expressed as:

$$K = \frac{M^2N}{\hat{M}^2\hat{N}} = \frac{M^2N}{\hat{M}\hat{N}} \cdot \frac{1}{\hat{M}} \cdot \rho_0 \tag{37}$$

It can be known from (37) that the transmitter can improve the coherent processing gain with a minimum division strategy by configuring the subarray with as many receive array elements as possible to achieve the diversity number [40].

4.3. Optimal Uniform Configuration for Hybrid Distributed PA-MIMO Radar System

Both the transmitter and the receiver sides are configured in a uniform non-overlapping manner. Hence, combining (17) and (27), we have:

$$\begin{cases} \Gamma\left(\frac{v_0}{2}, 2g_0\right) = \Gamma\left(\hat{N}\hat{M}, \frac{2NM^2\rho_0}{\hat{N}\hat{M}^2+NM^2\rho_0}\right) = \frac{NM^2\rho_0}{\hat{N}\hat{M}^2+NM^2\rho_0}\chi^2_{(2\hat{N}\hat{M})} & , \mathcal{H}_0 \\ \Gamma\left(\frac{v_1}{2}, 2g_1\right) = \Gamma\left(\hat{N}\hat{M}, \frac{2NM^2}{\hat{N}\hat{M}^2}\rho_0\right) = \frac{NM^2\rho_0}{\hat{N}\hat{M}^2}\chi^2_{(2\hat{N}\hat{M})} & , \mathcal{H}_1 \end{cases} \tag{38}$$

With the given radar system size $M \times N$, P_{FA} and ρ_0, we have:

$$P_{\mathrm{D-HPM}}(P_{\mathrm{FA}}) = 1 - Q_{\chi^2_{(2\hat{N}\hat{M})}}\left(\frac{Q^{-1}_{\chi^2_{(2\hat{N}\hat{M})}}(1-P_{\mathrm{FA}})\hat{N}\hat{M}^2}{\hat{N}\hat{M}^2 + NM^2\rho_0}\right) \tag{39}$$

(1) Model of **optimization problem 1**

The target detection probability will be improved by optimizing the configuration of the array elements, and it can be expressed as:

$$\begin{aligned} \mathcal{P}: \quad & [\hat{M}, \hat{N}] = \underset{M,N}{\arg\max}\left[1 - Q_{\chi^2_{(2\hat{N}\hat{M})}}\left(\frac{Q^{-1}_{\chi^2_{(2\hat{N}\hat{M})}}(1-P_{\mathrm{FA}})\hat{N}\hat{M}^2}{\hat{N}\hat{M}^2+NM^2\rho_0}\right)\right] \\ s.t. \quad & \mathcal{C}_1: \hat{M} \le \hat{N} \\ & \mathcal{C}_2: 1 \le \hat{M} \le M; \hat{M} \in \mathbb{Z} \\ & \mathcal{C}_3: 1 \le \hat{N} \le N; \hat{N} \in \mathbb{Z} \end{aligned} \tag{40}$$

(2) Model of **optimization problem 2**

Combining Equation (40) AND substituting $R_{E\max} = \sqrt[4]{\rho_0/\rho_{\min}}$ into the objective function, the configuration strategy for the **optimization problem 2** can be transformed into:

$$\begin{aligned} \mathcal{P}: \quad & [R_{E\max}] = \underset{M,N}{\arg\max}\left[\frac{NM^2\rho_0 Q^{-1}_{\chi^2_{(2\hat{N}\hat{M})}}(1-P_{\mathrm{D}})}{\hat{N}\hat{M}^2\left(Q^{-1}_{\chi^2_{(2\hat{N}\hat{M})}}(1-P_{\mathrm{FA}}) - Q^{-1}_{\chi^2_{(2\hat{N}\hat{M})}}(1-P_{\mathrm{D}})\right)}\right]^{\frac{1}{4}} \\ s.t. \quad & \mathcal{C}_1: \hat{M} \le \hat{N} \\ & \mathcal{C}_2: 1 \le \hat{M} \le M; \hat{M} \in \mathbb{Z} \\ & \mathcal{C}_3: 1 \le \hat{N} \le N; \hat{N} \in \mathbb{Z} \end{aligned} \tag{41}$$

(3) Model of **optimization problem 3**

The key part of this problem is to minimize the volume of the required equipment through the optimal array elements configuration while satisfying the intended target detection performance of the radar system. Clearly, the most intuitive and logical way to solve this problem is to increase system integration by sharing antenna transceivers in a time-sharing manner. Accordingly, the total volume of radar system equipment is:

$$\begin{aligned} \mathcal{P}: \quad & [M, N] = \underset{M,N}{\arg\max}\left[\frac{\hat{M}^3\left(Q^{-1}_{\chi^2_{(2\hat{M})}}(1-P_{\mathrm{FA}}) - Q^{-1}_{\chi^2_{(2\hat{M})}}(1-P_{\mathrm{D}})\right)}{\rho_0 Q^{-1}_{\chi^2_{(2\hat{M})}}(1-P_{\mathrm{D}})}\right]^{\frac{1}{4}} \\ s.t. \quad & \mathcal{C}_1: M = N \\ & \mathcal{C}_2: \hat{M} = \hat{N} \\ & \mathcal{C}_3: 1 \le \hat{M} \le M; \hat{M} \in \mathbb{Z} \\ & \mathcal{C}_4: 1 \le \hat{N} \le N; \hat{N} \in \mathbb{Z} \end{aligned} \tag{42}$$

4.4. QPSO-Based Stochastic Rounding Optimization Solution Algorithm

However, the optimization problem above is difficult to solve because it is an integer programming problem, which means its size is too large, and the computational effort is considerable if we just use the exhaustive search to find the optimal solution. Therefore, we propose a stochastic optimization rounding algorithm incorporating quantum-behaved particle swarm optimization (SR-QPSO) [41]. The particle swarm optimization algorithm with quantum behavior improves the algorithm to cover the whole search space during iteration by simulating the substantial uncertainty of state superposition in quantum

systems. Therefore, it improves the global search weakness at the tail end of the classical PSO algorithm search and enhances the global optimization capability of the algorithm [42].

In the SR-QPSO, to guarantee convergence of the swarm, each particle $P_{i,j}(t)$ must converge to its local attractor $p_i = (p_{i,1}, p_{i,2}, \ldots, p_{i,j}, \ldots, p_{i,D})$, $i = 1, 2, \ldots, N_{pop}$, which is expressed as:

$$p_{i,j}(t) = \frac{c_1 r_{1,j}(t) P_{i,j}(t) + (1 - c_2 r_{2,j}(t)) P_g(t)}{c_1 r_{1,j}(t) + c_2 r_{2,j}(t)} \tag{43}$$

where $P_g(t)$ represent the global best position of the population; c_1 and c_2, the acceleration coefficients, typically are both set to a value of 2.0; $r_{1,j}(t)$ and $r_{2,j}(t)$ are two random numbers uniformly distributed on the interval $(0, 1)$; D is the dimension of particle, and N_{pop} is the population size.

Moreover, the average optimal position coordinates in the evolution of the particle state are denoted as:

$$C(t) = (C_1(t), C_2(t), \ldots, C_j(t)) = (\frac{1}{N}\sum_{i=1}^{N} P_{i,1}(t), \frac{1}{N}\sum_{i=1}^{N} P_{i,2}(t), \ldots, \frac{1}{N}\sum_{i=1}^{N} P_{i,D}(t)) \tag{44}$$

And thus, using the Monte Carlo method, we can measure the j-th component of the position of the i-th particle at the $(t + 1)$-th using the following equation:

$$X_{i,j}(t+1) = p_{i,j}(t) \pm \frac{L_{i,j}(t)}{2} \cdot \ln(\frac{1}{u_{i,j}(t)}) \text{ , } u_{i,j}(t) \in \mathrm{U}(0, 1) \tag{45}$$

where $X_{i,j}(t)$ is the j-th component of the current position,

$$L_{i,j}(t) = 2 \cdot \alpha \cdot \left| C_j(t) - X_{i,j}(t) \right| \tag{46}$$

and the parameter α is set at 0.8 in this paper, which is defined as the contraction expansion (CE) coefficient.

Then, a random rounding method is adopted in which the fractional part of the particle position parameter is used as the probability value for upward rounding the parameter decimal part. Although the rounded problem is no longer equivalent to the original problem, the solution set of the original problem is included in the feasible solutions of the rounded optimization problem, i.e., the maximum value of the latter is not smaller than the maximum value of the original optimization problem. The entire algorithm flow is shown in Algorithm 1.

Algorithms 1: SR-QPSO

```
Initialization, set search dimensions D, population size W, and max iterations Q;
Disperse uniform random particles in [-X_max, X_max], record X_{i,t}^j;
Normalize the positional parameters of particles, probability rounded to decimals;
Calculate pbest P_{i,t}^j and gbest G_{i,t}^j;
Set the upper and lower bounds of the shrinkage factor α_0 and α_1;
WHILE not met iteration termination condition ε ≥ 1e-6 DO
    FOR t=1 TO Q DO
        Update contraction expansion factor;
        Calculate the average best individual position for iteration at t;
        FOR i=1 TO W DO
            Calculate and update particle positions X_{i,t}^j;
            IF X_{i,t}^j ∉ [-X_max, X_max], set X_{i,t+1}^j as boundary value;
            END IF
        END FOR
    END FOR
END WHILE
Update contraction expansion factor
```

5. Simulations and Analysis

5.1. Parameter Settings

In order to verify the effectiveness of the hybrid distributed PA-MIMO radar array configuration on target detection capability enhancement, some numerical simulations based on (40)–(42) are presented in this section. In the following, the defaulted radar system configuration parameters are $M = N = 100$, $P_{\mathrm{FA}} = 10^{-6}$, $\rho_0 = 6.0913 \times 10^7$ and the target RCS is $1\mathrm{m}^2$. In addition, the parameters of the SR-QPSO algorithm, i.e., the initial population size $W = 100$, the particle dimension $D = 2$, the max iterations $Q = 100$, and the upper bound of the particle position is 100 and the lower bound is 1.

5.2. Results and Discussion

We design some numerical experiments for the proposed closed-form approximations as (40)–(42), and the performance metrics adopted are listed as follows (Table 1).

Table 1. Applied performance metrics.

Names	Symbols	Settings
Detection Probability	P_{Dmax}	[0,1]
Effective Radar Range	$R_{E\mathrm{max}}$	$[0, +\infty]$
Number of array elements	M	[0,100]

(1) Case 1: Maximize Detection Probability

The convergence curve using the SR-QPSO to solve optimization problem 1 is shown in Figure 4. It indicates that the fitness function converges to 0.98 after about 16 iterations. And the corresponding optimal strategy for the array element configuration is $Opt\left(\hat{M}, \hat{N}\right) = (1, 13)$.

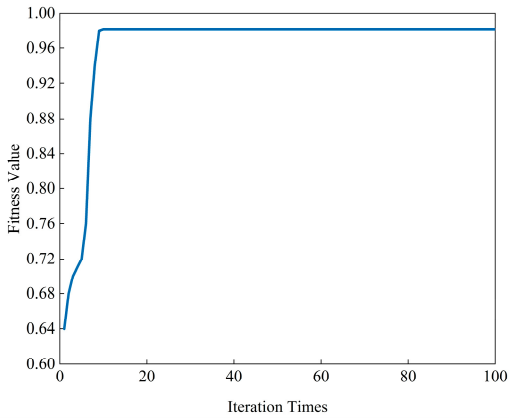

Figure 4. SR-QPSO convergence curve.

To verify that this configuration is not a local optimal solution, numerical simulations are carried out according to (40) in the following, with different transmitter diversity DOF $\hat{M}$, receiver diversity DOF $\hat{N}$ and P_{FA}. Then, the effect of the optimal configuration on the detection probability has been investigated and analyzed based on visualization.

First, we plotted the value of detection capability P_{D} of different $\hat{M}$ when $\hat{N}$ varying from 0 to 100 with the fixed $P_{\mathrm{FA}} = 10^{-6}$ in Figure 5. As can be observed, the value of $\hat{N}$ has a prominent influence on P_{D}. P_{D} will increase when $\hat{N}$ increase from 0 to about 5 or 13 when $\hat{M} = 1$. In contrast, P_{D} and $\hat{N}$ is negatively correlated in other situations. Besides, which is most important, the radar system with $\hat{M}$ greater than 1 has a much lower P_{D} than $\hat{M} = 1$, and the corresponding optimal transmitter side diversity DOF decreases as the receiving element volume increases, confirming the conclusion of Section 4.3 on transmitter diversity. Thus, subsequent experiments will not consider the case of $\hat{M} \geq 2$.

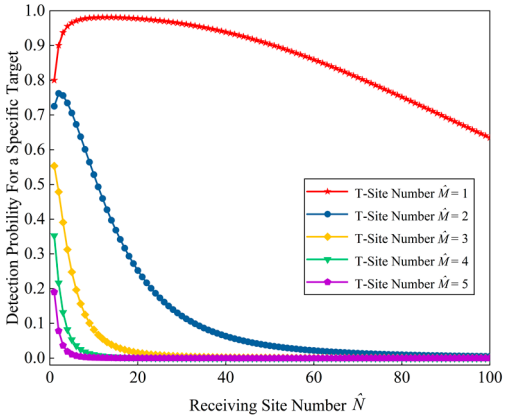

Figure 5. Optimal P_D versus receiver side diversity DOF.

Similarly, Figure 6 depicts $\hat{M}$'s effect on the detection probability P_D with different $\hat{N}$. As shown in Figure 6, the value of P_D significantly attenuates from 1 to almost 0 when $\hat{M}$ increases from 1 to 4. Essentially, this is because the diversity at the transmitter side reduces the coherent processing gain, while the contribution of the spatial diversity gain is much smaller than the coherent processing gain.

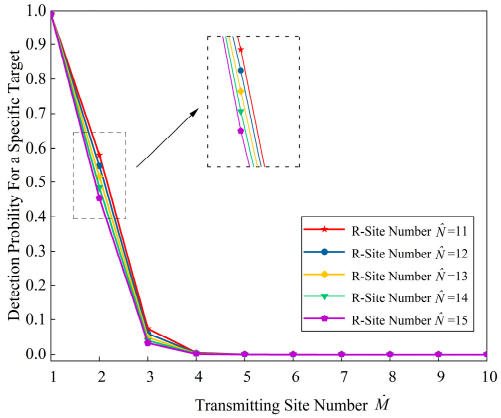

Figure 6. Optimal P_D versus transmitter side diversity DOF.

The analysis of Figures 5 and 6 reveals that the diversity at the receiver side can improve the detection performance only if the gain at the transmitter side meets a certain level.

Moreover, we could verify that (40) obeys the general rule that P_D positively correlated with P_{FA}, as shown in Figure 7.

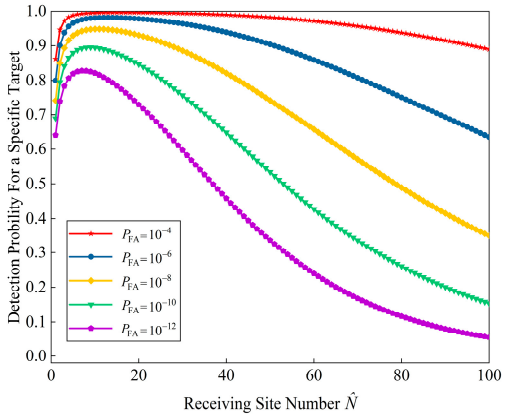

Figure 7. Impact of P_{FA} on optimal configuration.

(2) Case 2: Maximize Effective Radar Range

Assuming $P_{\mathrm{D}} = 0.8$, $P_{\mathrm{FA}} = 10^{-6}$ for the hybrid distributed PA-MIMO radar system, the SR-QPSO optimization is applied to solve **optimization problem 2** based on formula (42). The convergence of the fitness function is shown in Figure 8. With no more than 10 iterations, the effective range of the radar system $R_{E\max}$ converges to the optimum value of 1166.3 km. At this point, the optimal strategy for the array element configuration is $Opt\left(\hat{M}, \hat{N}\right) = (1, 5)$.

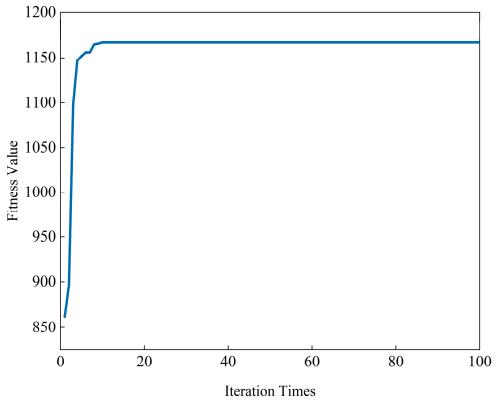

Figure 8. SR-QPSO convergence curve.

Then, four simulations are carried out to identify the effects of the transmitter side diversity DOF $\hat{M}$, the receiver side diversity DOF $\hat{N}$, P_{D} and P_{FA} on the effective range $R_{E\max}$ as shown in Figure 9, Figure 10, Figure 11, and Figure 12, respectively.

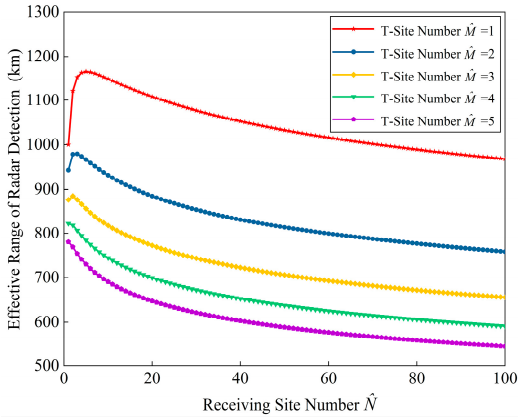

Figure 9. Optimal $R_{E\max}$ versus receiver side diversity DOF.

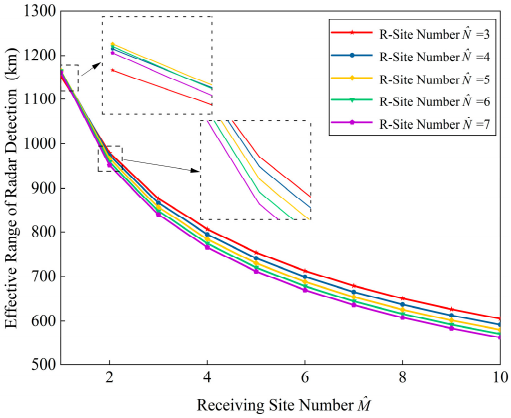

Figure 10. Optimal $R_{E\max}$ versus transmitter side diversity DOF.

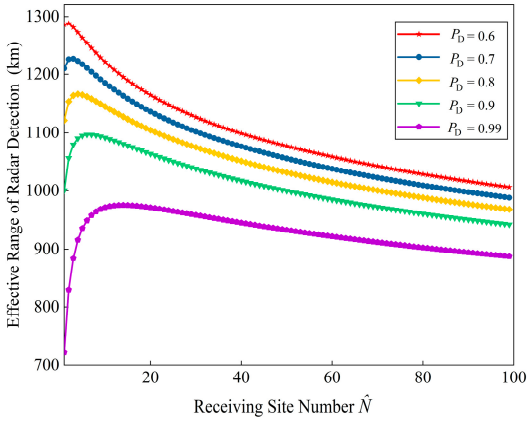

Figure 11. Impact of P_{D} on optimal configuration.

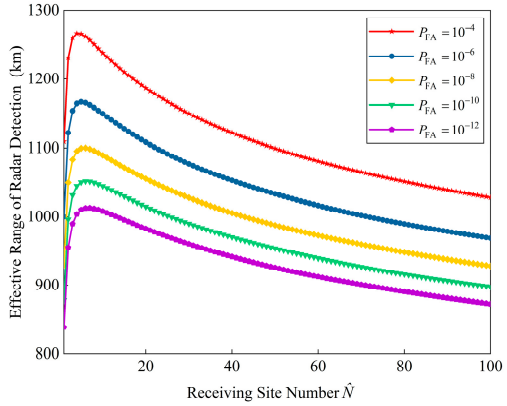

Figure 12. Impact of P_{FA} on optimal configuration.

In Figure 9, we let $\hat{M} = 1, 2, 3, 4, 5$ and draw the value of effective range when $\hat{N}$ varying in 1 and 100. It is clear that increasing the number of transmitter diversity DOF does not improve the range of the radar system compared to the optimal solution, but rather reduces the effective range. Moreover, the corresponding optimal transmit array division DOF for the transmit array division scheme decreases as the number of transmitter sites increases. This is still essentially a decrease in channel SNR due to transmitter side diversity. Therefore, the subsequent analysis will be based on the $\hat{M} = 1$.

In Figure 10, with fixed $\hat{N} = 3, 4, 5, 6, 7$, three curves of $R_{E\max}$ verses $\hat{M}$ are plotted according to (41), respectively. Varying $\hat{M}$, it was found that transmitter diversity also caused an attenuation of the effective range of the radar system. It can be observed that the optimal configuration strategy at the transmitter side for the condition $\hat{M} = 1$ is $\hat{N} = 5$, and for $\hat{M} = 2$ is $\hat{N} = 3$. Therefore, $\hat{M} = 1$ is not always the optimal transmitter-side diversity DOF for a certain $\hat{N}$ and the maximum benefit can only be achieved in coordination with the receiver-side array division.

In Figure 11, with the fixed $P_{\mathrm{FA}} = 10^{-6}$, the maximum effective range curves are calculated for the hybrid distributed PA-MIMO radar system with $P_{\mathrm{D}} = 0.6, 0.7, 0.8, 0.9, 0.99$. It can be obtained that as P_{D} increases, the effective action distance decreases accordingly. Secondly, the optimal receiver diversity DOF increases with the increase of the detection probability.

In Figure 12, the maximum effective range $R_{E\max}$ with $P_{\mathrm{FA}} = 10^{-4}, 10^{-6}, 10^{-8}, 10^{-10}, 10^{-12}$ are calculated for the hybrid distributed PA-MIMO radar system. Without loss of generality, the lower the false alarm probability P_{FA}, the shorter the effective range. By comparing with Figures 11 and 12, it shows that P_{FA} has less impact than P_{D} on effective range, but the optimal strategies $\hat{N}$ all increase as the detection accuracy rises.

(3) Case 3: Minimize System Element Volume

Based on the analysis in Case 1 and Case 2, we consider the hybrid distributed PA-MIMO radar with transceiver elements, which has the character $\hat{M} = \hat{N}$. Hence, (43) becomes a univariate objective function. Then the following two experiments are conducted to investigate the configuration optimization scheme based on the minimum amount of radar system element M (equal to N) with preset intended P_{FA} and P_{D}, respectively.

In Figure 13, the element volume of the radar system M curves versus system diversity $\hat{M}$. The optimal radar system design is given according to (42). Also, the result with respect to $P_{\mathrm{D}} = 0.6, 0.7, 0.8, 0.9, 0.99$ are all provided. Obviously, the higher the detection probability, the larger the amount of radar element required. When the P_{D} exceeds 0.8, the number of required T/R array elements first decreases and then increases with the number of division sites. Herein, the optimal division site number is 2. Conversely, when P_{D} is less than 0.8, the optimal array element configuration scheme is $\hat{M} = 1$. That is, the PA-MIMO is configured as a phased-array radar without diversity.

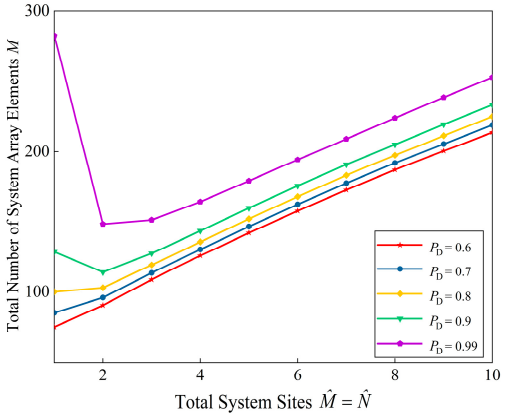

Figure 13. Impact of P_{D} on optimal configuration.

Figure 14 shows curves of the total volume of the radar system M versus system diversity $\hat{M}$. The optimal radar system design is given according to (42). Also, the result concerning $P_{\mathrm{FA}} = 10^{-4}, 10^{-6}, 10^{-8}, 10^{-10}, 10^{-12}$ are all provided. The lower the false alarms probability, the greater the amount of radar system equipment required. Furthermore, the scheme $\hat{M} = 2$ makes the system equipment volume the smallest when P_{FA} is less than 10^{-10}. And the optimal array configuration $\hat{M} = 1, 2$ minimized the M when $P_{\mathrm{FA}} = 10^{-10}$. However, when the P_{FA} is greater than 10^{-10}, the optimal array configuration scheme is phased array radar.

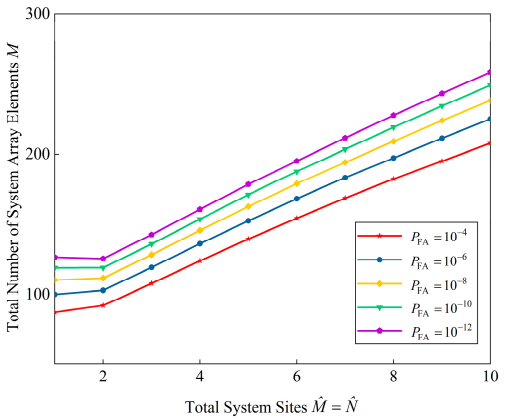

Figure 14. Impact of P_{FA} on optimal configuration.

6. General Discussion

From the folloeing simulation results in Table 2, the following general conclusions can be drawn for the hybrid distributed PA-MIMO radar system.

Table 2. Quantitative results.

Simulation	Optimal Index	Configuration Scheme	Convergence Time
Case 1	$P_{\mathrm{Dmax}} = 0.98$	$(\hat{M}, \hat{N}) = (1, 13)$	87.275 s
Case 2	$R_{E\mathrm{max}} = 1166.3$ km	$(\hat{M}, \hat{N}) = (1, 5)$	86.778 s
Case 3	$M, \hat{M}$	depend on P_{FA} and P_{D}	/
MIMO radar	$P_{\mathrm{D}} = 0.63, R_E = 1006$ km	$(\hat{M}, \hat{N}) = (100, 100)$	/
PA radar	$P_{\mathrm{D}} = 0.80, R_E = 1000$ km	$(\hat{M}, \hat{N}) = (1, 1)$	/

(1) With the increase in diversity DOFs at the transmitter and receiver, the radar detection performance deteriorates when DOFs exceed the optimal values. Generally, different optimization objectives have different optimal configuration schemes, and the radar detection probability and false alarm probability also affect the value of optimal diversity DOF $\hat{M}$ and $\hat{N}$.

(2) The essence of the superior detection performance of the hybrid distributed PA-MIMO radar lies in the coherent processing improves the local SNR within each subarray, based on which the spatial diversity gain generated between the independent subarrays will further improve the target detection capability. In particular, for all optimization problems, only a small transmitter-side diversity DOF is required since the gain generated by transmit-side diversity cannot compensate for the lost coherent processing gain.

(3) The results show that the optimal scheme of configuration is M = 1, N = 13 in the case of optimal detection probability, and the detection probability reaches 0.98; while the optimal configuration strategy is M = 1, N = 5 for maximizing the effective radar range to 1166.9 km. When the array transceiver is shared, the minimum number of elements is needed when only one phased array antenna is used under the condition of $P_{\mathrm{D}} \leq 0.8$. Further, it is necessary to divide the array elements into two separated phased array antennas to obtain the spatial diversity gain when $P_{\mathrm{D}} > 0.8$. Hence, optimized array element configuration improves target detection performance to some extent.

(4) In this paper, as a further extension of [20], the optimal allocation of coherent processing gain and spatial diversity gain is conducted. However, the paper is limited to the optimal configuration under uniform division of array elements, which is obviously far from the optimal array element allocation scheme and needs to be studied in depth in the future.

7. Conclusions

This paper investigates the optimal array elements configuration scheme for hybrid distributed PA-MIMO radar based on target detection. Its essence is to change the coherence between the array signals through the array elements configuration, to coordinate the proportion of the coherence gain and the spatial diversity gain in the radar system, and to ultimately improve the target detection performance of the radar system without increasing resources. And the SR-QPSO method is proposed to solve the optimal array element configuration scheme. From the analysis in the paper, it is clear that neither distributed MIMO radar nor phased-array radar merely using diversity gain or coherent processing gain is optimal. Therefore, the system SNR is improved by coherent processing at the transmitter side, and the target detection performance will be further optimized by diversity gain at the receiver side based on a certain SNR ratio level. The optimized detection probability reaches 0.98, the effective distance of radar action reaches 1166.3 km, and the minimum number of array elements of the system is 2. Compared with other configuration

schemes, the obtained optimal configuration strategy has a significant improvement on the target detection performance. The limitation is that the configuration strategy is based on the uniform division of the array elements and does not fully utilize the optimization potential of the array element configuration. Therefore, the theoretical derivation and numerical results confirm the effectiveness of the hybrid distributed PA-MIMO array element configuration in improving the target detection capability of the radar system, and the obtained conclusions are of reference value for the system configuration and practical application of PA-MIMO radar.

We note that this work is based on the condition of the fixed noise background. Future works might concern the influence of clutters and cognitive interference [43] and try to realize dynamic optimization management with high detection accuracy [44]. In addition, other approaches for optimization may be taken into account, such as reinforcement learning algorithm [45,46] and game theory [47].

Author Contributions: C.Q. proposed the conceptualization and methodology. C.Q. wrote the draft manuscript. H.Z. and J.X. supervised the experimental analysis and revised the manuscript. X.Y. and Z.D. made contributions to the software. All authors have read and agreed to the published version of the manuscript.

Funding: This research was funded by the National Natural Science Foundation of China, grant number 62001506.

Conflicts of Interest: The authors declare no conflict of interest.

References

1. Fishler, E.; Haimovich, A.; Blum, R.; Chizhik, D.; Cimini, L.; Valenzuela, R. MIMO radar: An idea whose time has come. In Proceedings of the 2004 IEEE Radar Conference (IEEE Cat. No.04CH37509), Philadelphia, PA, USA, 29–29 April 2004; pp. 71–78.
2. Shi, C.; Wang, Y.; Salous, S.; Zhou, J.; Yan, J. Joint Transmit Resource Management and Waveform Selection Strategy for Target Tracking in Distributed Phased Array Radar Network. *IEEE Trans. Aerosp. Electron. Syst.* **2021**, *58*, 2762–2778. [CrossRef]
3. Shi, C.; Wang, Y.; Wang, F.; Salous, S.; Zhou, J. Joint Optimization Scheme for Subcarrier Selection and Power Allocation in Multicarrier Dual-Function Radar-Communication System. *IEEE Syst. J.* **2020**, *15*, 947–958. [CrossRef]
4. Malanowski, M.; Kulpa, K. Detection of Moving Targets With Continuous-Wave Noise Radar: Theory and Measurements. *IEEE Trans. Geosci. Remote Sens.* **2012**, *50*, 3502–3509. [CrossRef]
5. Van Trees, H.L. *Detection, Estimation And Modulation Theory*; Wiley: New York, NY, USA, 1968.
6. Zhu, Z.; Kay, S.; Raghavan, R.S. Information-Theoretic Optimal Radar Waveform Design. *IEEE Signal Process. Lett.* **2017**, *24*, 274–278. [CrossRef]
7. Yan, J.; Liu, H.; Pu, W.; Zhou, S.; Liu, Z.; Bao, Z. Joint Beam Selection and Power Allocation for Multiple Target Tracking in Netted Colocated MIMO Radar System. *IEEE Trans. Signal Process.* **2016**, *64*, 6417–6427. [CrossRef]
8. Xu, L.; Li, J.; Stoica, P. Target detection and parameter estimation for MIMO radar systems. *IEEE Trans. Aerosp. Electron. Syst.* **2008**, *44*, 927–939.
9. Zhang, H.; Liu, W.; Shi, J.; Fei, T.; Zong, B. Joint Detection Threshold Optimization and Illumination Time Allocation Strategy for Cognitive Tracking in a Networked Radar System. *IEEE Trans. Signal Process.* 2022; 1–15, *to be published*.
10. Zhang, H.; Liu, W.; Zhang, Z.; Lu, W.; Xie, J. Joint Target Assignment and Power Allocation in Multiple Distributed MIMO Radar Networks. *IEEE Syst. J.* **2021**, *15*, 694–704. [CrossRef]
11. Zhang, H.; Zhou, H.; Zong, B.; Xie, J. A Fast Power Allocation Strategy for Multibeam Tracking Multiple Targets in Clutter. *IEEE Syst. J.* **2021**, *16*, 1249–1257. [CrossRef]
12. Yan, J.; Dai, J.; Pu, W.; Liu, H.; Greco, M.S. Target Capacity Based Resource Optimization for Multiple Target Tracking in Radar Network. *IEEE Trans. Signal Process.* **2021**, *69*, 2410–2421. [CrossRef]
13. Yan, J.; Liu, H.; Jiu, B.; Chen, B.; Liu, Z.; Bao, Z. Simultaneous Multibeam Resource Allocation Scheme for Multiple Target Tracking. *IEEE Trans. Signal Process.* **2015**, *63*, 3110–3122. [CrossRef]
14. Qi, C.; Xie, J.; Zhang, H. Joint Antenna Placement and Power Allocation for Target Detection in a Distributed MIMO Radar Network. *Remote Sens.* **2022**, *14*, 2650. [CrossRef]
15. Li, J.; Stoica, P. MIMO Radar with Colocated Antennas. *IEEE Signal Process. Mag.* **2007**, *24*, 106–114. [CrossRef]
16. Haimovich, A.M.; Blum, R.S.; Cimini, L.J. MIMO radar with widely separated antennas. *IEEE Signal Process. Mag.* **2007**, *25*, 116–129. [CrossRef]
17. Fishler, E.; Haimovich, A.; Blum, R.; Cimini, L.; Chizhik, D.; Valenzuela, R. Spatial Diversity in Radars—Models and Detection Performance. *IEEE Trans. Signal Process.* **2006**, *54*, 823–838. [CrossRef]
18. Zhang, G.Y. *Principle of Phased Array Radar*; National Defense Industry Press: Beijing, China, 2009.

19. Skolnik, M.I. *Radar Handbook*; McGraw-Hill Book Co.: New York, NY, USA, 1990.
20. Xu, J.; Dai, X.-Z.; Xia, X.-G.; Wang, L.-B.; Yu, J.; Peng, Y.-N. Optimizations of Multisite Radar System with MIMO Radars for Target Detection. *IEEE Trans. Aerosp. Electron. Syst.* **2011**, *47*, 2329–2343. [CrossRef]
21. Brookner, E. Phased-Array and Radar Breakthroughs. In Proceedings of the 2007 IEEE Radar Conference, Waltham, MA, USA, 17–20 April 2007; pp. 37–42.
22. Brookner, E. Phased-array and radar astounding breakthroughs—An update. In Proceedings of the 2008 IEEE Radar Conference, Rome, Italy, 26–30 May 2008; pp. 1–6.
23. Butt, A.; Naqvi, I.H.; Riaz, U. Hybrid Phased-MIMO Radar: A Novel Approach With Optimal Performance Under Electronic Countermeasures. *IEEE Commun. Lett.* **2018**, *22*, 1184–1187. [CrossRef]
24. Shi, C.; Ding, L.; Wang, F.; Salous, S.; Zhou, J. Joint Target Assignment and Resource Optimization Framework for Multitarget Tracking in Phased Array Radar Network. *IEEE Syst. J.* **2021**, *15*, 4379–4390. [CrossRef]
25. Hassanien, A.; Vorobyov, S.A. Phased-MIMO Radar: A Tradeoff Between Phased-Array and MIMO Radars. *IEEE Trans. Signal Process.* **2010**, *58*, 3137–3151. [CrossRef]
26. Bergin, J.; McNeil, S.; Fomundam, L.; Zulch, P.A. MIMO Phased-Array for SMTI Radar. In Proceedings of the 2008 IEEE Aerospace Conference, Big Sky, MT, USA, 1–8 March 2008.
27. Ismail, N.E.-D.; Mahmoud, S.H.; Hafez, A.S.; Reda, T. A new phased MIMO radar partitioning schemes. In Proceedings of the IEEE Aerospace Conference, Cincinnati, OH, USA, 19–23 May 2014; pp. 1–7.
28. ADeligiannis, A.; Amin, M.; Lambotharan, S.; Fabrizio, G. Optimum Sparse Subarray Design for Multitask Receivers. *IEEE Trans. Aerosp. Electron. Syst.* **2019**, *55*, 939–950. [CrossRef]
29. Yi, J.; Wan, X.; Leung, H.; Lu, M. Joint Placement of Transmitters and Receivers for Distributed MIMO Radars. *IEEE Trans. Aerosp. Electron. Syst.* **2017**, *53*, 122–134. [CrossRef]
30. Radmard, M.; Chitgarha, M.M.; Majd, M.N.; Nayebi, M.M. Antenna placement and power allocation optimization in MIMO detection. *IEEE Trans. Aerosp. Electron. Syst.* **2014**, *50*, 1468–1478. [CrossRef]
31. Brookner, E. Never ending saga of phased array breakthroughs. In Proceedings of the 2010 IEEE International Symposium on Phased Array Systems and Technology, Waltham, MA, USA, 12–15 October 2010; pp. 61–73.
32. Fei, T.; Tan, X.; Zhang, K.; Wang, P.; Wang, H. Optimizations of Elements Configurations for Distributed MIMO Digital Array Radar. *Mod. Radar* **2017**, *39*, 22–27.
33. Fei, T.; Tan, X.; Lin, Q.; Qu, Z. Research on detection performance for distributed MIMO digital array radar. *J. Huazhong Univ. Sci. Technol.* **2017**, *45*, 80–85.
34. Zhou, S.; Liu, H.; Zhao, Y.; Hu, L. Target spatial and frequency scattering diversity property for diversity MIMO radar. *Signal Process.* **2011**, *91*, 269–276. [CrossRef]
35. Zhang, H.; Shi, J.; Zhang, Q.; Zong, B.; Xie, J. Antenna Selection for Target Tracking in Collocated MIMO Radar. *IEEE Trans. Aerosp. Electron. Syst.* **2021**, *57*, 423–436. [CrossRef]
36. Jaynes, E.T.; Bretthorst, G.L. Probability theory: The logic of science. *Math. Intell.* **2005**, *27*, 83.
37. Box, G.E.P. Some Theorems on Quadratic Forms Applied in the Study of Analysis of Variance Problems, I. Effect of Inequality of Variance in the One-Way Classification. *Ann. Math. Stat.* **1954**, *25*, 290–302. [CrossRef]
38. Stolkin, R.; Florescu, I. Probability of Detection and Optimal Sensor Placement for Threshold Based Detection Systems. *IEEE Sens. J.* **2009**, *9*, 57–60. [CrossRef]
39. Zhang, T.; Xia, Z.; Yang, Y.; Zhao, Z.; Liu, X.; Zhang, Y.; Liu, D.; Yin, X. Waveform Optimization of High SNR and High Resolution Cognitive Radar for Sparse Target Detection. In Proceedings of the 2021 IEEE 4th International Conference on Electronics Technology (ICET), Chengdu, China, 7–10 May 2021; pp. 200–203.
40. Xu, J.; Dai, X.-Z.; Xia, X.-G.; Wang, L.-B.; Yu, J.; Peng, Y.-N. Optimal transmitting diversity degree-of-freedom for statistical MIMO radar. In Proceedings of the 2010 IEEE Radar Conference, Arlington, VA, USA, 10–14 May 2010; pp. 437–440.
41. Jun, S.; Wenbo, X.; Bin, F. A global search strategy of quantum-behaved particle swarm optimization. *IEEE Conf. Cybern. Intell. Syst.* **2004**, *1*, 111–116.
42. Jun, S.; Wenbo, X.; Bin, F. Adaptive parameter control for quantum-behaved particle swarm optimization on individual level. *IEEE Int. Conf. Syst. Man Cybern.* **2005**, *4*, 3049–3054.
43. Yao, Y.; Liu, H.; Miao, P.; Wu, L. MIMO Radar Design for Extended Target Detection in a Spectrally Crowded Environment. *IEEE Trans. Intell. Transp. Syst.* **2021**, 1–10. [CrossRef]
44. Zhang, W.; Shi, C.; Salous, S.; Zhou, J.; Yan, J. Convex Optimization-Based Power Allocation Strategies for Target Localization in Distributed Hybrid Non-Coherent Active-Passive Radar Networks. *IEEE Trans. Signal Process.* **2022**, *70*, 2476–2488. [CrossRef]
45. Deng, M.; Cheng, Z.; He, Z. Limited-Memory Receive Filter Design for Massive MIMO Radar in Signal-Dependent Interference. *IEEE Signal Processing Lett.* **2022**, *29*, 1536–1540. [CrossRef]
46. Ahmed, A.M.; Ahmad, A.A.; Fortunati, S.; Sezgin, A.; Greco, M.S.; Gini, F. A Reinforcement Learning Based Approach for Multitarget Detection in Massive MIMO Radar. *IEEE Trans. Aerosp. Electron. Syst.* **2021**, *57*, 2622–2636. [CrossRef]
47. Nguyen, H.T.; Hoang, D.T.; Luong, N.C.; Niyato, D.; Kim, D.I. A Hierarchical Game Model for OFDM Integrated Radar and Communication Systems. *IEEE Trans. Veh. Technol.* **2021**, *70*, 5077–5082. [CrossRef]